J. Embryol. exp. Morph. **92**, 145–164 (1986)
Printed in Great Britain © *The Company of Biologists Limited 1986*

The role of glycosaminoglycans in anuran pigment cell migration

R. P. TUCKER
Department of Zoology, University of California, Davis, CA 95616, USA

SUMMARY

The migratory pathways of neural crest-derived pigment cells were examined in two anurans, *Xenopus laevis* and *Discoglossus pictus*, and correlated with the distribution of glycosaminoglycans (GAG) in the extracellular matrix (ECM) of these pathways. In *Xenopus*, melanophores in the trunk reach the dermis by initially migrating ventrally, between the neural tube and somites, and then by migrating through the somites to reach the subectodermal space. In *Discoglossus*, melanophores, iridophores, and xanthophores migrate laterally over the dorsal margin of the somites to reach the dermis. GAG was identified in the light microscope using alcian blue staining and in the electron microscope using ruthenium red staining. The ECM at the dorsal entrance to the lateral pathway in *Xenopus* and in young *Discoglossus* (at a stage prior to invasion by pigment cells) is filled with 25–50 nm chondroitin sulphate proteoglycan aggregates. When this ECM in *Xenopus* is digested *in vivo* with chondroitinase ABC, melanophores enter the lateral pathway. In older *Discoglossus* embryos, the migration of pigment cells into the lateral pathway is correlated with increases in the space between the ectoderm and somites and in the number of hyaluronate microfibrils. These observations suggest that chondroitin sulphate proteoglycan in the subectodermal ECM restricts the migration of pigment cells into the lateral pathway by limiting the amount of space for migration and possibly by acting as a less adhesive migratory substratum than the ventral pathway, and that in *Discoglossus* hyaluronate opens spaces permitting the migration of pigment cells directly over the dorsal margin of the somites.

INTRODUCTION

The trunk neural crest is a population of cells that arises from or near the dorsal surface of the neural tube during or soon after the fusion of the neural folds. As development proceeds, these cells disperse along one of three major pathways: laterally, between the ectoderm and the somites; ventrally, between the neural tube and the somites; and, in amphibians, dorsally into the dorsal fin (for reviews see Hörstadius, 1950; Weston, 1980; Le Douarin, 1982; Erickson, 1986). The neural crest differentiates into a variety of cell types, including the neurones and accessory cells of the peripheral nervous system, as well as the pigment cells (DuShane, 1935; Stevens, 1954). Amphibian pigment cells include black melanophores, yellow xanthophores, and iridophores, which contain reflecting platelets (Bagnara *et al.* 1979).

The role of the extracellular matrix (ECM) in controlling neural crest morphogenesis has received considerable attention. The work of Weston & Butler

Key words: neural crest, pigment cells, extracellular matrix, glycosaminoglycans, hyaluronate, *Xenopus laevis, Discoglossus pictus*.

(1966), Le Douarin & Teillet (1974), and Noden (1975) established that the extracellular environment is responsible for defining the migratory pathways and, in part, the differentiative pathways of neural crest cells. ECM macromolecules that have been identified in neural crest migratory pathways include: glycosaminoglycans (GAG), especially hyaluronate (HA) and chondroitin sulphate (CS; Pratt, Larsen & Johnston, 1975; Derby, 1978; Pintar, 1978); collagen (von der Mark, von der Mark & Gay, 1976; Hay, 1978; Löfberg, Ahlfors & Fällström, 1980); and fibronectin (FN; Newgreen & Thiery, 1980; Mayer, Hay & Hynes, 1981; Duband & Thiery, 1982; Thiery, Duband & Delouvée, 1982). Efforts to determine the roles of these macromolecules in neural crest morphogenesis have consisted largely of confronting neural crest cells *in vitro* with known concentrations and combinations of isolated ECM components in the culture medium, bound to two-dimensional substrata (Fisher & Solursh, 1979; Newgreen *et al.* 1982; Rovasio *et al.* 1983; Erickson & Turley, 1983), or within three-dimensional collagen gels (Tucker & Erickson, 1984). Others have attempted to modify the ECM or ECM–cell interactions by injection of hyaluronidase (Anderson & Meier, 1982) or competitive synthetic peptides (Boucaut *et al.* 1984). The behaviour and morphology of neural crest cells *in vitro* correlates well with what is known about the binding interactions between the various ECM components and ECM–cell interactions (Turley, Erickson & Tucker, 1985). Of particular interest to the present study, HA has been shown to promote neural crest cell migration through relatively dense collagen gels *in vitro*, apparently by opening spaces in the matrix (Tucker & Erickson, 1984). HA has been implicated in opening spaces and permitting neural crest cell migration *in vivo* as well, for example, during the early migration of avian cranial neural crest cells (Pratt *et al.* 1975) as well as later in development when neural crest-derived fibroblasts invade the HA-rich collagenous stroma of the cornea (Toole & Trelstad, 1971). Also, CS proteoglycan is a relatively non-adhesive substratum for neural crest cells *in vitro* (Newgreen *et al.* 1982; Erickson & Turley, 1983), and avian neural crest cells avoid regions containing high concentrations of CS proteoglycan *in situ* (Newgreen *et al.* 1982).

This study combines an analysis of the distribution of a subpopulation of the amphibian neural crest, the pigment cells, with changes in the distribution of ECM macromolecules *in vivo*. Amphibian embryos are particularly well suited for such a study: the ectoderm is relatively transparent, making direct observation of the pigment cells possible; the embryos are accessible and amenable to surgical manipulation; and the ECM is extensive at a relatively early stage in development. Using time-lapse micrography, histological preparations, and *in vivo* enzymic digestion of ECM, this study demonstrates that the pathways that amphibian pigment cells follow to the dermis are correlated with the distribution of GAG.

MATERIALS AND METHODS

Xenopus laevis embryos were obtained from artificial fertilizations using gametes from adults maintained in a colony at Davis. Jelly was removed from embryos by brief treatment with 2 % cysteine (pH 8·0), and the fertilization envelope was removed manually. Adult *Discoglossus*

pictus were kindly provided by C. Campanella (Naples, Italy). *Discoglossus* gametes were obtained using the methods of Campanella & Gabbiani (1980), and fertilized artificially. *Discoglossus* and *Xenopus* embryos were maintained in 20 % Steinberg's solution or tap water at 21 °C until used.

The appearance of melanophores in *Xenopus* was observed using a Nikon Diaphot inverted microscope and was recorded by taking photographs at 3 h intervals and by time-lapse videomicrography. Embryos were illuminated from the side with a fibre optics light source (Dyonics), and anaesthetized, if necessary, by adding a few crystals of ethyl m-aminobenzoate (Sigma) to the saline solution. Recordings were made with an RCA or MTI video camera, and a Panasonic time-lapse videotape player.

Identification of pigment cells

Melanophores were identified in whole mounts and serial sections prepared for light microscopy (LM; see below) as black cells, and in the transmission electron microscope (TEM) as cells containing numerous electron-dense melanosomes. Iridophores appeared lustrous silver or gold when viewed in whole mounts with epi-illumination, and in the TEM these cells contained distinctive oblong platelets. The distribution of xanthophores was determined in whole mounts by using NH_4OH-induced autofluorescence of pteridines (Epperlein & Claviez, 1982*a*). In brief, anaesthetized embryos were placed in 10 % NH_4OH, mounted on a glass slide, and viewed with a Zeiss epifluorescence microscope equipped with 365 nm excitation and 395 nm barrier filters. Xanthophores fluoresce bluish-white under these conditions. This method is specific for xanthophores, since iridophores are distinct when viewed simultaneously by shining white light onto the stage from the side, and since in older *Discoglossus* larvae only cells that were yellowish when viewed with bright field optics fluoresced. Xanthophores were also identified by the presence of characteristic pterinisomes in the TEM.

Surgical manipulations

All surgical manipulations were carried out in 100 % Steinberg's solution with penicillin (75 i.u. ml^{-1}), streptomycin (75 $\mu g\,ml^{-1}$) and Fungizone (2·5 $\mu g\,ml^{-1}$) on sterile agar or wax-coated dishes. Melanophore tissue affinities were determined by peeling the ectoderm away from the somites with tungsten needles. The underlying pigment cells either remained attached to the somites or were attached to the ectoderm.

To digest GAG in the lateral migratory pathway of *Xenopus*, a U-shaped incision was made through the ectoderm over the anterior regions of the flank of stage-30 (for *Xenopus* stages see Nieuwkoop & Faber, 1956) embryos while the embryo was immersed either in 1 i.u. ml^{-1} chondroitinase ABC (CH ABC; Seikagaku Kogyo) in enriched Tris buffer (pH 7·4; Saito, Yamagata & Suzuki, 1968) or in enriched Tris buffer alone. The ectoderm was then peeled back toward the dorsal midline until the neural tube was exposed. After 30 min at 30 °C, the embryos were transferred to 100 % Steinberg's solution for 12 h at 21 °C, and the resulting melanophore pattern was observed. Embryos with disrupted patterns were fixed and processed for TEM (see below).

Identification of matrix components

To identify GAG in the ECM of *Xenopus* embryos, specimens of various ages were fixed in 10 % formalin in phosphate-buffered saline (PBS) with or without 0·5 % cetylpyridinium chloride (CPC; Polysciences) overnight at room temperature. Embryos were subsequently dehydrated in ethanol, cleared in xylene, and embedded in Paraplast (Lancer). Specimens were then sectioned at 7 μm, hydrated, and either stained with 0·1 % toluidine blue or treated with 5 M-HCl for 30 sec and stained with 1 % alcian blue in 0·025 M-$MgCl_2$ (pH 2·6) overnight. In some cases, alternate sections were digested with CH ABC in enriched Tris buffer (pH 8·0), enriched Tris buffer alone, 100 TRU ml^{-1} *Streptomyces* hyaluronidase (ST HY; Seikagaku Kogyo) in acetate buffer (pH 5·8), or acetate buffer alone for 3 h at 37 °C before alcian blue staining. 7-day-old *Discoglossus* embryos (at a stage when the pigment cells were just visible through the ectoderm) were also prepared for alcian blue staining, although sections were not treated with enzyme.

The identity and distribution of extracellular matrix materials were determined in the TEM using methods modified from Hay & Meier (1974) and Turley *et al.* (1985). In order to determine the morphological appearance of individual ECM macromolecules, matrix components (human umbilical cord HA, 2 mg ml^{-1}, Sigma; rat chondrosarcoma CS proteoglycan, 3 mg ml^{-1}, a gift from J. Stevens in the laboratory of V. C. Hascall) were added individually or together to collagen gels (Vitrogen, 750 $\mu g\,ml^{-1}$, Flow) prepared according to Elsdale & Bard (1972). The gels were then fixed with 2·5 % glutaraldehyde and 1·5 % paraformaldehyde in 0·1 M-sodium cacodylate buffer at pH 7·4 containing 0·1 % ruthenium red (RR, Polysciences; Luft, 1971) and 0·1 % tannic acid (TA, Fisher; Singley & Solursh, 1980) overnight at 4 °C. After washing in buffer, the gels were postfixed for 1 h at room temperature in 1 % OsO_4 containing RR (Luft, 1971), rinsed, dehydrated in ethanol, and embedded in Epon–Araldite. Specimens were sectioned and stained with uranyl acetate and lead citrate, and observed with a Philips 410 electron microscope.

Xenopus and *Discoglossus* embryos containing neural crest cells before and during migration were prepared in a similar fashion. Specimens were fixed overnight at 4 °C in 2 % glutaraldehyde in PBS with either 0·1 % TA, 0·1 % RR, or both stains. Specimens were cut transversely with a razor blade after 30 min in the fixative to facilitate penetration of the stains. After a sodium cacodylate buffer rinse, specimens were postfixed in 1 % OsO_4 in 0·1 M-sodium cacodylate saturated with RR (if RR was present in the primary fixative). Specimens were then embedded as outlined above, and sectioned at 5 μm to a depth of 50 μm from the cut surface. The last thick section was stained in 0·05 % toluidine blue and coverslipped for reference and camera-lucida sketching. The block was then trimmed and thin sectioned for transmission electron microscopy. To check the specificity of the RR stain for GAG, and to aid in the identification of matrix components, the ECM of stage-33 *Xenopus* embryos and 2-week-old *Discoglossus* larvae was digested with GAG-specific enzymes prior to RR staining using methods modified from Hay & Meier (1974). In brief, specimens were fixed 1 h in 10 % formaldehyde at 4 °C, rinsed four times in PBS, and cut transversely with a razor blade while incubating in ST HY (100 TRU ml^{-1}) in acetate buffer (pH 5·8), acetate buffer alone, CH ABC (1 i.u. ml^{-1}) in enriched Tris buffer (pH 8·6), or enriched Tris buffer alone. Specimens were exposed to buffer or enzyme for 2 h at 37 °C. Following treatment, the specimens were rinsed with PBS and prepared for TEM using the methods outlined above. The specificity of the enzymes used in this study was determined by digesting known samples of HA and CS (shark cartilage, Sigma) in appropriate buffers and analysing the digestion products by cellulose acetate electrophoresis. Under these conditions, ST HY in acetate buffer (pH 5·8) specifically digests HA, and digestion with CH ABC in enriched Tris buffer (pH 8·6) is specific for CS. At pH 8·0 CH ABC digestion is less specific for sulphated GAG (Derby & Pintar, 1978).

RESULTS

Pigment cell pattern formation

(1) Xenopus laevis

Melanophores become externally visible in *Xenopus* embryos at stage 33 (40–48 h). Lightly pigmented cells are initially seen along the dorsal surface of the neural tube, especially in the anterior half of the embryo, as well as over the dorsal portion of the yolky endoderm in the lateral plate mesoderm (the sheet of mesoderm surrounding the endoderm). Time-lapse videomicrography of the development of this pigment pattern shows that occasionally a lightly pigmented cell reaches the lateral plate mesoderm by migrating through the intersomitic furrows (two cases in five specimens). The migration of most melanophores to the lateral plate mesoderm, however, is restricted to the ventral migratory pathway where they are not externally visible. These melanophores probably remain

invisible because of incomplete melanization and the opacity of the young embryo due to the presence of yolk platelets in the somites and ectoderm.

By stage 39 (2·5 days), a well-defined pattern of dark melanophores is seen (Fig. 1A), and the distribution of these cells is easily determined by optical sectioning through the transparent tissues. Melanophores in the trunk are found in two dorsal stripes, one along the dorsal margin of the somites, and another along the surface of the neural tube, visible through the somites. Melanophores are also visible ventrally in the lateral plate mesoderm, as well as associated with the pronephric duct and tubules. In the tail (i.e. posterior to the endoderm), pigment cells are seen along the ventral margins of the notochord and somites. Melanophores are only rarely encountered in the dorsal and ventral fins, or over the surface of the somites.

NH_4OH-induced fluorescence of pteridines reveals a few xanthophores beneath the ectoderm over the lateral plate mesoderm (which contains melanophores) in two of the four stage-39 embryos examined. No xanthophores were found using NH_4OH treatment in embryos younger than stage 39. By stage 41, NH_4OH-induced fluorescence reveals xanthophores over the somites dorsal to the gut where melanophores are rarely seen, as well as scattered beneath the ectoderm over the somites in the tail (Fig. 2A). The number of cells that autofluoresce when exposed to NH_4OH is highly variable, even among siblings, with some animals totally lacking positive cells, and others having approximately equal numbers of fluorescing cells and melanophores in the tail region. Fluorescing cells were typically rounded or fragmented by NH_4OH treatment, although occasionally cells with a branched morphology similar to many of the melanophores were seen.

At stage 45 (4 days; Fig. 1B), melanophores are still visible along the dorsal apex of the somites and neural tube, as well as over the surface of the somites throughout the tail. The surface of the somites dorsal to the gut remains relatively free of melanophores, as does the ventral-most portion of the lateral plate mesoderm. Iridophores are found in the eye and in the lateral plate mesoderm at this stage, although xanthophores are not externally visible.

(2) Discoglossus pictus

Discoglossus embryos are opaque due to the presence of maternal pigmentation in the ectoderm during the stages of development when melanophores differentiate (Fig. 1C). As development proceeds, maternal pigment gradually disappears so that by 5 days after fertilization melanophores are externally visible. Melanophores are found in two configurations: either individually scattered over the surface of the somites and gut, or in a continuous, branching network beneath the ectoderm throughout the embryo. Individual melanophores are not seen in the fins, and are more commonly encountered near the neural tube and the dorsal portion of the somites than more ventral regions. By 6–7 days iridophores are also externally visible. These cells are seen near the dorsal surface of the neural tube, over the surface of the somites, gut, and head, as well as in the dorsal and ventral tail fins. By 8 days (Fig. 1D) xanthophores are also externally visible, with a

distribution similar to iridophores. This was confirmed with observations of larvae following NH_4OH treatment (Fig. 2B). Melanophores are frequently found associated with capillaries in the subectodermal space, whereas iridophores are not.

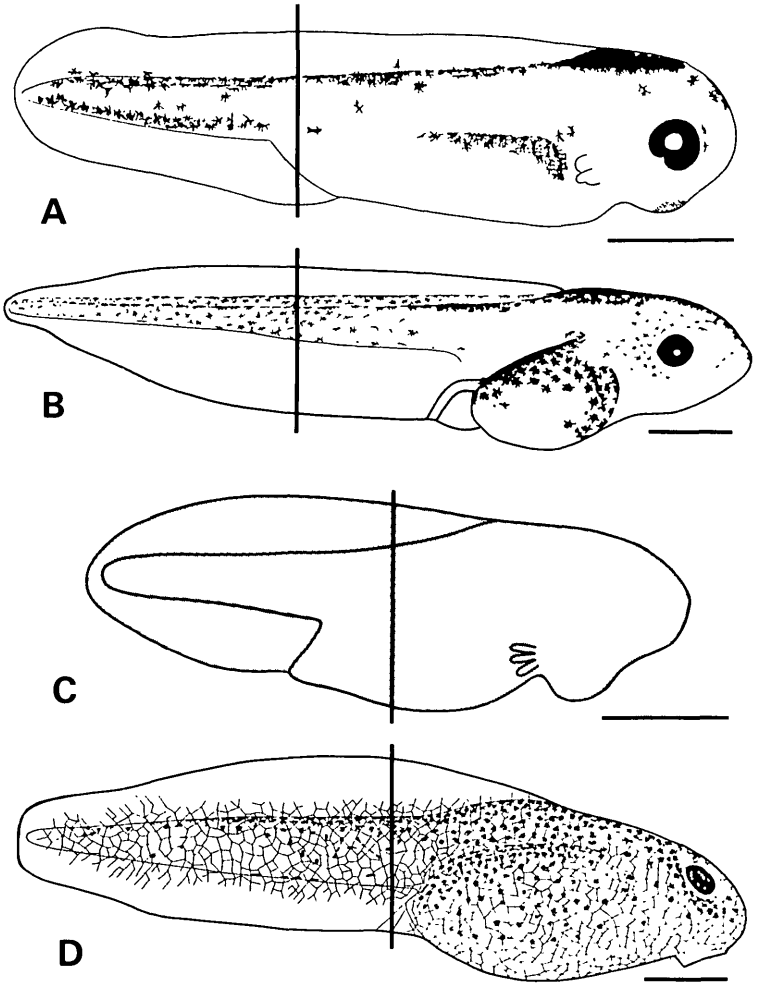

Fig. 1. (A) The distribution of melanophores in *Xenopus laevis* (stage 39). Melanophores are found along the dorsal margin of the somites, the dorsal portion of the neural tube, as well as ventrally in the lateral plate mesoderm and near the ventral margin of the somites in the tail. Melanophores are rarely encountered in the dorsal and ventral fins as well as in the subectodermal space (except in the head). The vertical bar indicates the axial level of Fig. 3A. (B) The distribution of melanophores in *Xenopus* at stage 45. Note that melanophores are now seen in the dermis of the tail. The vertical bar marks the approximate axial level examined in Fig. 4. (C) *Discoglossus pictus* 4 days after fertilization. The appearance of melanophores is obscured by maternal pigmentation. The vertical bar indicates the axial level of Fig. 3B. (D) *Discoglossus* at 8 days. Melanophores are visible in the dorsal region in the subectodermal space both as individual cells associated with the somites and blood vessels, as well as in a network associated with the epidermal basement membrane. The vertical bar indicates the axial level of Fig. 3C. Bars equal 1 mm.

Pathways of pigment cell migration

(1) Xenopus laevis

Fig. 3A is a camera-lucida drawing of a cross section showing the distribution of melanophores in the posterior trunk (some endoderm is present ventrally) of a stage-39 *Xenopus* embryo. At this axial level, melanophores are found along the dorsal surface of the neural tube, as well as along the ventral migratory pathway. Melanophores are seen next to the notochord, and further ventrally on the medial surface of the somites. Melanophores are seen neither in the lateral pathway beneath the ectoderm, nor in the fin mesenchyme. Similarly, at more anterior levels, melanophores are observed in the ventral and not the lateral pathway. Melanophores enter the lateral plate mesoderm from the ventral pathway, where they intermingle with mesoderm cells, and are only occasionally observed directly beneath the ectoderm. Melanophores are frequently associated with the ducts and tubules of the pronephros. The distribution of melanophores seen in serial sections, together with time-lapse observations of melanophore pattern development, strongly suggest that the initial pathway the melanophores use during migration is ventrally between the neural tube and somites, and not laterally, beneath the ectoderm (Fig. 3D).

After migrating ventrally, melanophores in *Xenopus* migrate through the somites to reach the subectodermal space. Melanophores *en route* from the ventral pathway to the dermis through the somites are illustrated in Fig. 4. By focusing through the somites of fixed or anaesthetized *Xenopus* larvae (stage 45; Fig. 4A–C), some melanophores are seen in the intersomitic furrows, and others are

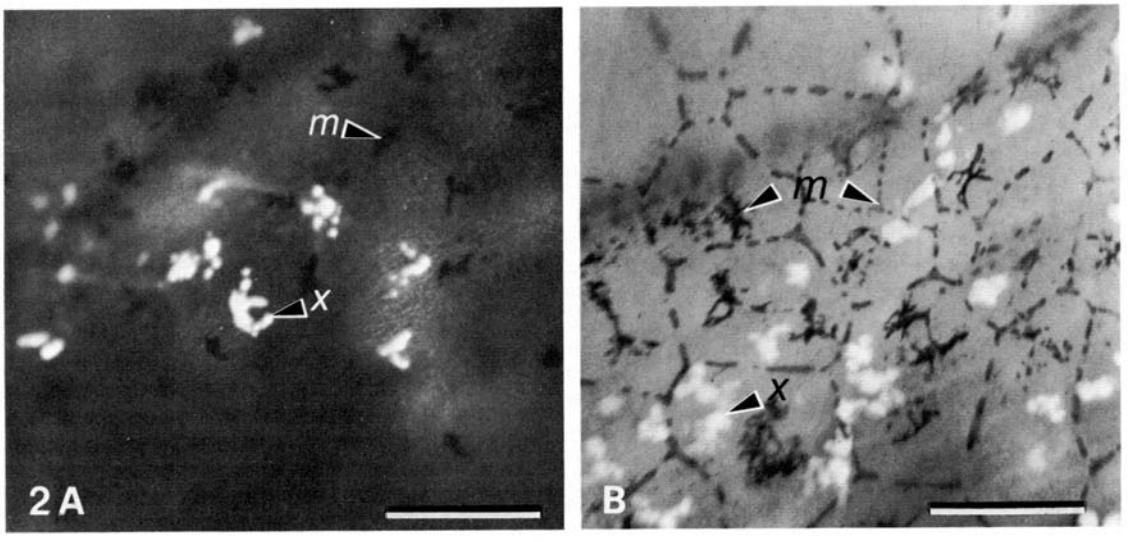

Fig. 2. (A) Xanthophores (*x*) in the tail of a stage-41 *Xenopus laevis* larva revealed by the autofluorescence of pteridines. Melanophores (*m*) are also visible. (B) Xanthophores (*x*) and melanophores (*m*) in the tail of an 8-day-old *Discoglossus* larva. Bars equal 200 μm.

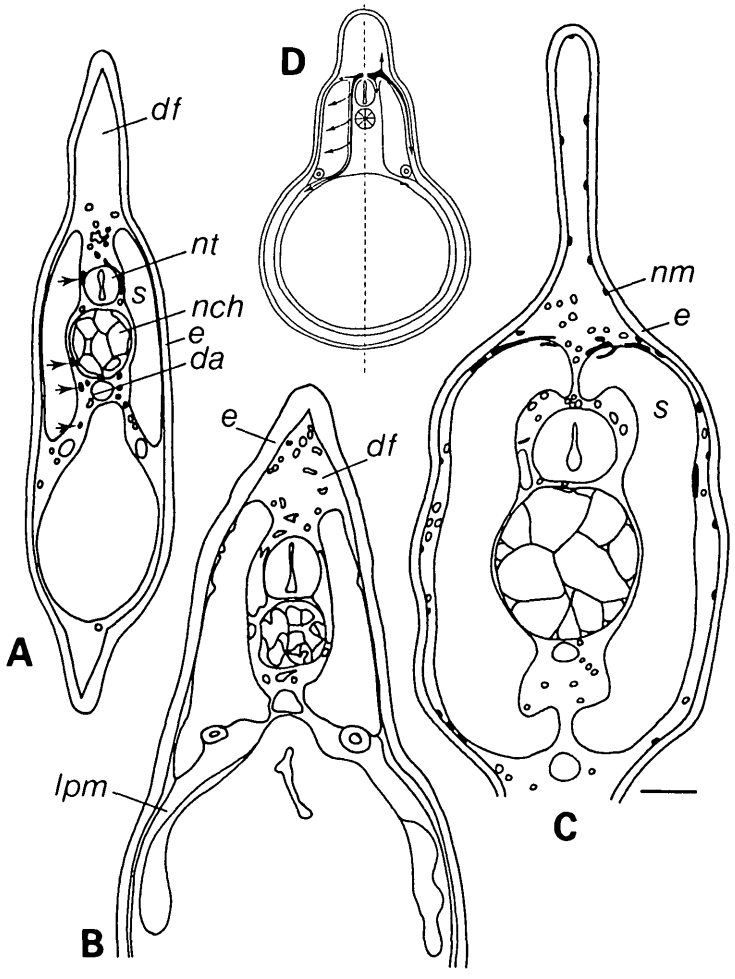

Fig. 3. (A) Camera-lucida drawing of a cross section through the trunk of a stage-39 *Xenopus laevis* embryo. Melanophores (black, arrowheads) are seen near the neural tube (*nt*) and in the ventral pathway between the somites (*s*) and the notochord (*nch*) and dorsal aorta (*da*). There are no pigment cells in the dorsal fin (*df*). Note the close apposition between the somites and ectoderm (*e*). (B) Camera-lucida sketch of a cross section through the trunk of a 4-day-old *Discoglossus pictus* embryo. Melanophores are not visible yet at this axial level. The dorsal fin (*df*) contains numerous mesenchymal cells. There is little space between the somites and ectoderm (*e*). The lateral plate mesoderm (*lpm*) surrounds the endoderm. (C) Camera-lucida drawing of a cross section through an 8-day-old *Discoglossus* larva showing melanophores (black) in the lateral pathway. Melanophores forming the network seen in Figs 1D and 2B (*nm*) are associated with the ectoderm (*e*). A large space filled with mesenchymal cells (including pigment cells) is seen between the somites (*s*) and ectoderm (*e*). See Fig. 1A–D for reference. (D) Diagrammatic representation of the migratory pathways taken by melanoblasts and melanophores in *X. laevis* (left) and *D. pictus* (right). Bar equals 100 μm, A–C.

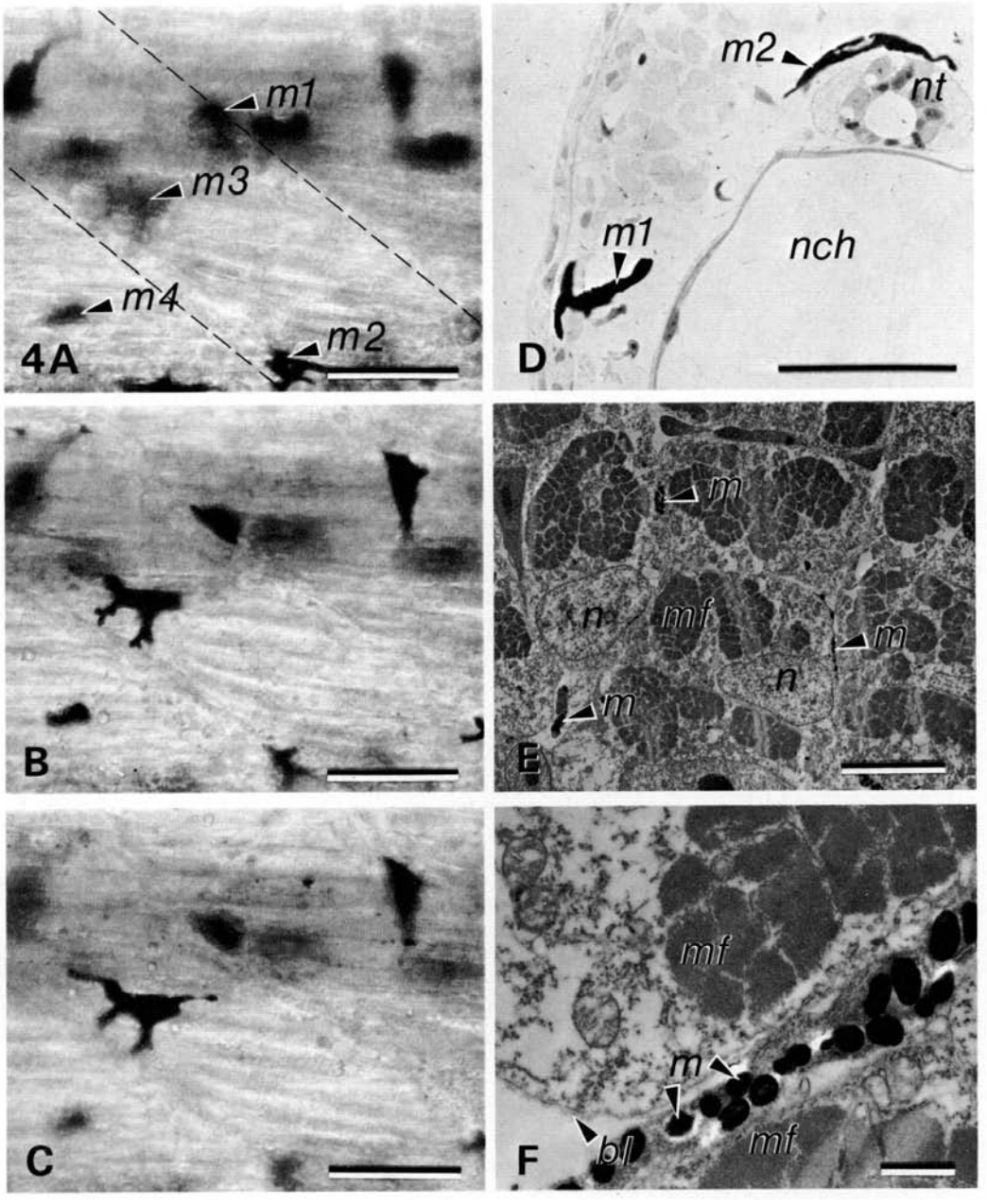

Fig. 4. (A–C) Through-focus series through the somites of a stage-45 *Xenopus laevis* larva. Intersomitic furrows are indicated by dashed lines in Fig. 4A. Melanophores are found in the intersomitic furrows (*m1, m2*) as well as between striated muscle cells of individual somites (*m3, m4*). (D) 5 μm-thick section through the tail of a stage-45 *Xenopus* showing a melanophore (*m1*) leaving the ventral pathway and spreading in the subectodermal space. Another melanophore (*m2*) is associated with the neural tube (*nt*), which is dorsal to the notochord (*nch*). (E) Low-magnification TEM showing melanophore processes (*m*) within the somites of a stage-45 *Xenopus* larva. Note the muscle cell nuclei (*n*) and the bundles of myofibrils (*mf*). ×1600. (F) Higher-magnification TEM of a melanophore process containing melanosomes (*m*) between two muscle cells containing myofibrils (*mf*). Note the basal lamina-like material (*bl*) surrounding the muscle cell. ×10 400. Bars equal A–D, 50 μm; E, 10 μm; F, 1 μm.

seen sending processes between the striated muscle cells of a single somite. Thick sections through the tail show melanophores leaving the ventral pathway between somite cells and spreading into the subectodermal space (Fig. 4D). TEM of thin sections through the tail (Fig. 4E,F) reveals numerous melanophore processes between the striated muscle cells of the somite. The migration of melanophores through this tissue coincides with the appearance of patches of basal lamina around the muscle cells.

(2) Discoglossus pictus

At 4 days, melanophores are just appearing in the head of *Discoglossus*. Cross sections through the trunk of these embryos reveal numerous unpigmented cells, probably neural crest cells, in the dorsal fin mesenchyme and in the ventral pathway (Fig. 3B). The former population of cells probably contain pigment cell precursors, and the latter neuronal precursors. There appear to be few mesenchymal cells in the subectodermal space. As development proceeds (8 days), however, melanophores are found in the lateral pathway, associated with the basement membrane of the ectoderm (these are the melanophores in the continuous network) as well as along the outer surface of the somites and associated with capillaries (Fig. 3C,D). Melanophores are also seen associated with the pronephric ducts.

(3) *Extracellular spaces*

In the sections represented in Fig. 3, it is apparent that the size of the extracellular space is correlated with the presence or absence of melanophores. This is true in specimens embedded in plastic for light and electron microscopy, as well as in paraffin sections. In *Xenopus*, where melanophores are restricted to the ventral pathway, the somite and the ectoderm are very tightly apposed (4–5 μm); the space is no greater than one cell diameter. In contrast, in older (8-day) *Discoglossus*, there is a much larger space between the ectoderm and somites (10–50 μm), and many pigment cells as well as other mesenchymal cells are present. This subectodermal space is frequently filled with several layers of cells, suggesting that the differences in the observed size of the subectodermal space in *Xenopus*, 4-day-old *Discoglossus*, and 8-day-old *Discoglossus*, represent actual differences in the size of this space *in vivo*, and are not principally artifacts of dehydration and embedding.

Distribution of ECM

(1) *Alcian blue staining*

Alcian blue stains fibrillar material in the dorsal fin mesenchyme of *Xenopus* (stage 40) and 6-day-old *Discoglossus*, as well as the basement membrane underlying the ectoderm over the surface of the somites. In *Xenopus*, the staining is most intense under the ectoderm of the fin and near the dorsal margin of the somite, as well as along the ventral portion of the neural tube and around the

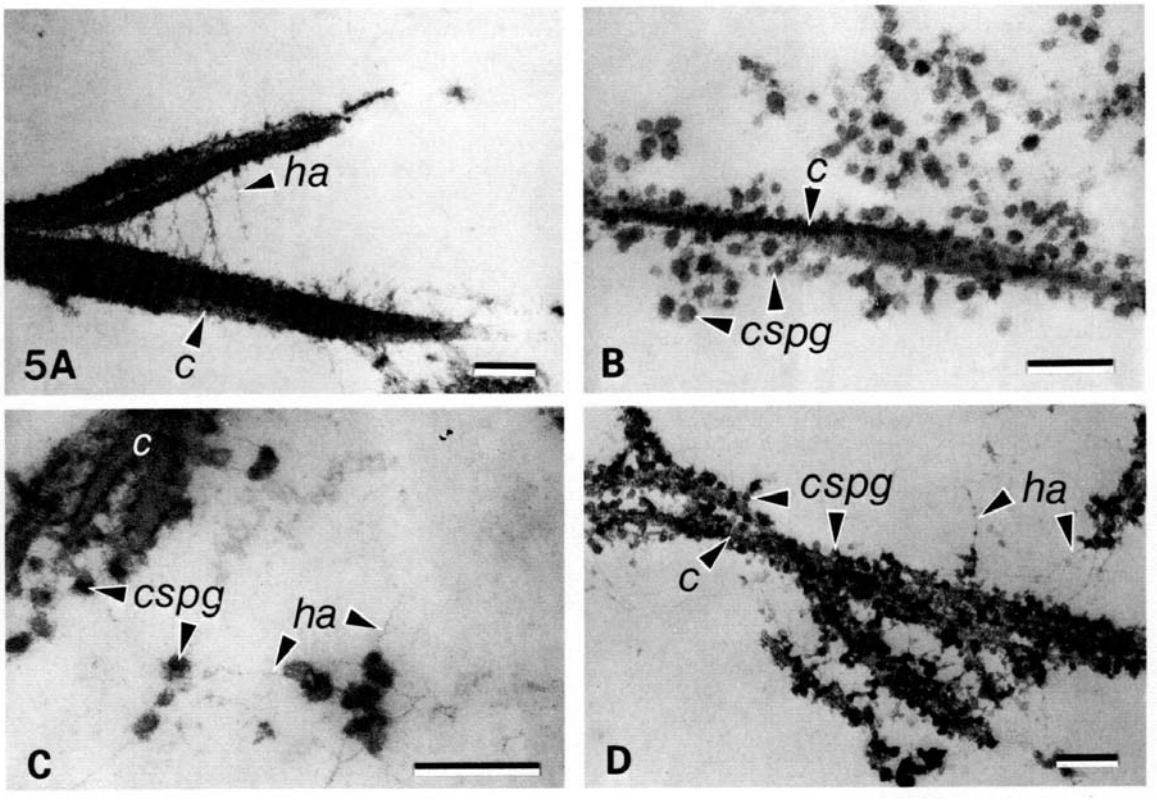

Fig. 5. (A) TEM of a collagen gel containing HA and stained with RR. Microfibrils (*ha*) are seen between the collagen fibres (*c*). ×38 000. (B) TEM of a collagen gel containing CS proteoglycan. 25–50 nm spherical aggregates (*cspg*) are seen associated with collagen fibres (*c*). ×54 800. (C) TEM of a collagen (*c*) gel containing CS proteoglycan (*cspg*) and HA (*ha*). ×82 000. (D) ECM from the region between the neural tube and notochord of a 12-day *Discoglossus pictus* larva. 25–50 nm spherical aggregates (*cspg*) are associated with collagen fibres (*c*) and microfibrils (*ha*). Microfibrils were sensitive to digestion with ST HY, and the number of CS proteoglycan aggregates was reduced following CH ABC digestion. ×38 000. Bars equal 200 nm.

notochord. The latter regions stain the most intensely in *Discoglossus* as well. The alcian blue appears to stain GAG primarily, because both the absence of CPC in the fixative and digestion of the sections with CH ABC and ST HY reduces the staining considerably. Since digestion with either enzyme results in similar overall reduction of staining in *Xenopus*, the morphology of the ECM when observed in the TEM was used to identify individual GAG.

(2) *Identification of GAG using ruthenium red (RR) staining*

Fig. 5 shows the morphology of artificial ECM containing known matrix components prepared for TEM using RR and TA fixation, and a portion of the ECM from between the notochord and neural tube of *Discoglossus*. In both the artificial ECM and ECM *in situ* collagen fibres can be identified by their characteristic repeating striations. When HA and collagen alone are present in the

artificial matrix (Fig. 5A), microfibrils 2–4 nm in diameter are seen between collagen fibres. These microfibrils are similar in morphology to 3–4 nm microfibrils that have been shown to be sensitive to hyaluronidase digestion by other investigators (Hay, 1978). When CS proteoglycan is added to the collagen gel, spherical aggregates 25–50 nm in diameter are seen associated with the collagen fibres (Fig. 5B). When both HA and CS proteoglycan are added to the same gel (Fig. 5C), the spherical aggregates are seen associated with both microfibrils and the collagen fibrils, in a manner resembling ECM *in situ* (Fig. 5D). In both artificial ECM and ECM *in situ,* microfibrils and spherical aggregates are not seen if RR is omitted from the fixative. The number of spherical aggregates seen in *Xenopus* ECM is reduced after digestion of the specimen with either CH ABC or ST HY (perhaps due to an association between the HA and CS proteoglycan), and in *Discoglossus* ECM the number of microfibrils is reduced following ST HY treatment, and not by CH ABC treatment. Based on these results, together with the identification of ECM by other researchers following specific digestions (Hay & Meier, 1974; Hay, 1978), HA is identified in the electron micrographs as unstriated 1–5 nm microfibrils, and CS proteoglycan as 25–50 nm spherical aggregates.

(3) Xenopus *ECM in the TEM*

At stage 40, the subectodermal pathway near the dorsal margin of the somites of *Xenopus* contains numerous CS proteoglycan aggregates associated with unorganized collagen fibrils and the ectodermal basal lamina (Fig. 6A,E). CS proteoglycan coats the collagen fibrils in this space at all stages examined (stages 30–45), although at stage 30, when the neural crest has begun to disperse, there is less CS proteoglycan than at later stages. The lateral surface of the somites is free of RR-staining material. HA microfibrils are rarely observed in the lateral pathway of *Xenopus*. It is also interesting to note that in the ventral pathway, near the neural tube, there is considerably less CS proteoglycan lining the collagen fibrils than in the lateral pathway of the same specimen.

(4) Discoglossus *ECM in the TEM*

In *Discoglossus* embryos prior to the appearance of melanophores (3 and 4 days), the ECM of the lateral pathway is strikingly similar to the ECM of the lateral pathway of *Xenopus* embryos (Fig. 6B). CS proteoglycan aggregates line the dermal collagen fibrils and the basal lamina of the ectoderm. However, HA microfibrils are seen in the lateral pathway more frequently than in *Xenopus*, especially near the surface of the somites. In older larvae (8 and 14 days), the lateral pathway contains a lattice of collagen fibrils in the ectodermal basement membrane, with some RR-staining material associated with the collagen. Between the collagen and somites the space is filled with microfibrils and associated CS proteoglycan (Fig. 6C). Fig. 6D,E compare the morphologies of the ECM in the lateral pathways of *Discoglossus* and *Xenopus*, respectively, at high magnification.

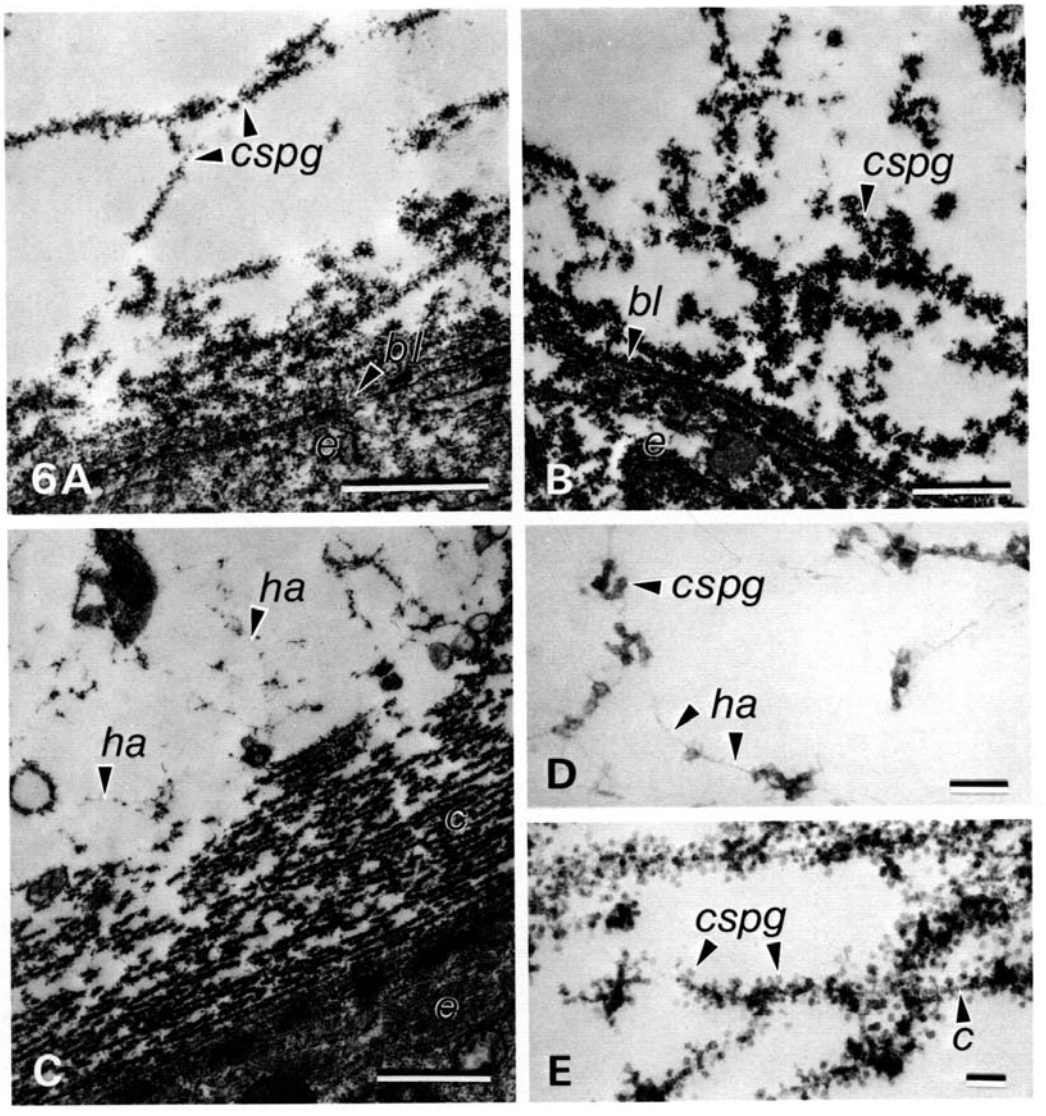

Fig. 6. (A) ECM of the dorsal lateral pathway of *Xenopus laevis*, stage 40. CS proteoglycan aggregates (*cspg*) line collagen fibres and the basal lamina (*bl*) underlying the ectoderm (*e*). ×21 000. (B) ECM of the lateral pathway of a 4-day-old *Discoglossus pictus* embryo. Spherical aggregates (*cspg*) are associated with collagen fibres and the basal lamina (*bl*) underlying the ectoderm (*e*). ×14 000. (C) ECM between the ectoderm (*e*) and somites of a 8-day-old *Discoglossus* larva contains numerous microfibrils (*ha*). Microfibrils and spherical aggregates are associated with the collagen fibres (*c*) of the dermis. ×16 900. (D) Higher magnification of the ECM seen in Fig. 6C. Spherical aggregates (*cspg*) are associated with microfibrils (*ha*). Note the similarity to Fig. 5C. ×82 000. (E) Higher magnification of the ECM seen in Fig. 6A. Spherical aggregates (*cspg*) are associated with striated collagen fibres (*c*). Note the absence of microfibrils and the similarity to Fig. 5B. ×54 800. Bars equal A–C, 1 μm; D,E, 100 nm.

The apparent increase in the concentration of HA microfibrils is correlated with the opening of spaces between the somites and the ectoderm in *Discoglossus*.

(5) *Pigment cell–tissue affinities*

Melanophores are occasionally seen in the lateral pathway of *Xenopus* during the early stages of pattern formation, especially in the intersomitic furrows. When the overlying ectoderm is peeled away using tungsten needles from an anaesthetized embryo, these melanophores remain attached to the surface of the somites. This suggests that somites rather than ectoderm were being used as the migratory substrata. Similarly, in older embryos that have more melanophores as well as xanthophores in the dermis, nearly all of the pigment cells remain associated with somites and not the ectoderm, as determined by NH_4OH treatment of peeled-away ectoderms. In contrast, when the ectoderm is peeled away from the lateral suface of a 7-day-old *Discoglossus* embryo, individual melanophores and iridophores remain associated with the somites and ectoderm in approximately equal numbers. The affinity of xanthophores in *Discoglossus* was not determined.

(6) *Digestion of GAG* in vivo

12 h after exposing stage-30 *Xenopus* embryos (early neural crest dispersal) to CH ABC for 30 min, an altered pigment pattern was observed in two of the four embryos (Fig. 7). In these cases, up to 10 melanophores were found in the lateral pathway, and the dorsal fin was greatly reduced at the site of the operation. In the two treatment cases that developed normally (no melanophores in the lateral

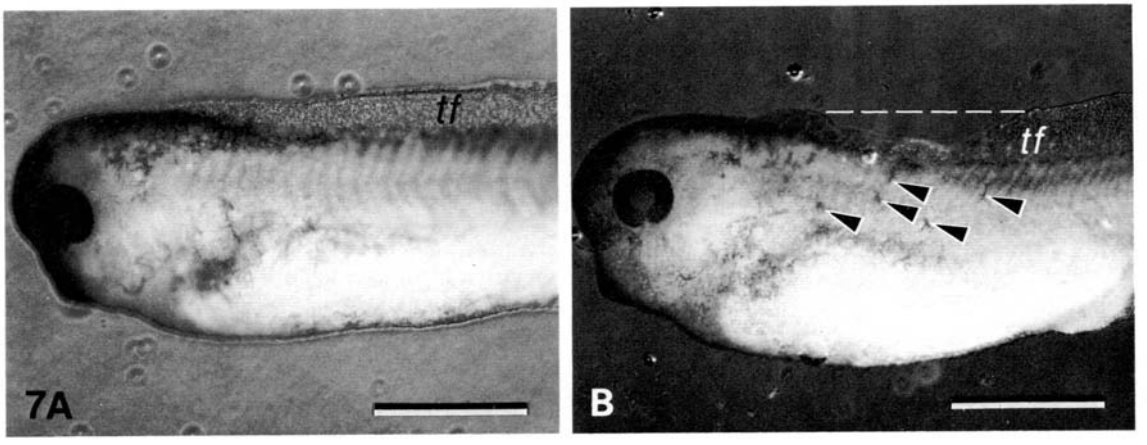

Fig. 7. (A) *Xenopus laevis* embryo 12 h after exposing the ECM of the lateral pathway to Tris buffer. Note the normal tail fin (*tf*) and the absence of melanophores over the surface of the somites. (B) *Xenopus laevis* embryo 12 h after exposing the ECM of the lateral pathway to CH ABC in Tris buffer. Note the disruption of the tail fin (*tf*) near the operation (dashed line) and the melanophores (arrows) that are now in the lateral pathway. Bars equal 1 mm.

pathway), the dorsal fin was also normal, suggesting that the incision had not exposed the entrance of the lateral pathway to the enzyme. All four control animals developed normal pigment patterns, as did the unoperated side of the two treated embryos displaying an abnormal distribution of melanophores. Thick sections through the region of CH ABC digestion showed that a large space had formed beneath the ectoderm on the treatment side and not on the control side of the embryo, suggesting that adhesion between the ectoderm and somite was reduced. Thin sections stained with RR did not reveal a gross difference in the number of CS proteoglycan aggregates in the digested lateral pathway ECM and in the control subectodermal ECM. This observation suggests that the GAG was replenished during the 12 h following disruption of the pathway.

DISCUSSION

In *Xenopus laevis*, the major migratory pathway of neural crest-derived melanoblasts is ventral, between the neural tube and somites. This was determined by the study of melanophore pattern formation in embryonic stages with easily recognizable differentiated melanophores using time-lapse video and serial section histological analysis. Melanophores in the tail eventually reach the dermis by migrating through the somites, either through the furrows or around individual somitic muscle cells. The predominant use of the ventral pathway by melanophores in *Xenopus* was suggested by MacMillan (1976), who grafted homotopically [^{3}H]thymidine-labelled neural crest into unlabelled hosts and observed in the anterior region of the trunk that labelled nuclei were found exclusively in the ventral and dorsal (tail fin) pathways. MacMillan's (1976) observations suggest that all neural crest-derived cells, including iridoblasts and xanthoblasts, reach the peritoneum or dermis by migrating through the ventral pathway. Since morphological markers for iridophores and xanthophores appear relatively late in development, the early migratory pathways of these cells could not be determined directly in this study. However, xanthophores first appeared beneath the dermis at the stage when melanophores had also reached the dermis by migrating through the somites. This suggests that xanthophores may use the same pathway as the melanophores. In *Discoglossus pictus*, the early migrations of pigment cells could not be observed directly due to the opacity of the embryo. However, at later stages when pigment cells were visible beneath the ectoderm, it was apparent that iridophores, xanthophores, and melanophores (or their unpigmented precursors) reached the dermis by migrating over the apex of the somites into the lateral pathway. Migration through the lateral pathway appears to be the predominant method for pigment cells to reach the dermis. This is the migratory pathway in a number of urodeles, including the axolotl (Dalton, 1950; Keller & Spieth, 1984), *Taricha torosa, T. granulosa*, and *T. rivularis* (Twitty, 1936; Twitty & Bodenstein, 1939), and *Triturus alpestris* (Epperlein & Claviez, 1982*a*,*b*).

Using ruthenium red staining, which also can be combined with enzyme digestions to identify GAG, Löfberg & Ahlfors (1978) and Löfberg *et al.* (1980)

have conducted detailed studies of the ECM surrounding migrating neural crest cells in the axolotl. They observed an increase in space between the neural tube, somites, and ectoderm filled with RR-positive fibrils at the time of initial neural crest migration. When observed in the TEM, this RR-positive ECM contained striated collagen fibrils coated with 25–30 nm spherical aggregates as well as microfibrils. Thus the axolotl appears to be similar to *Discoglossus* in that microfibrils, which probably represent HA (Turley *et al.* 1985), appear concurrently with the opening of spaces between tissues and the migration of the neural crest into the lateral pathway.

The appearance of HA during the opening of extracellular spaces has been reported in a number of embryonic tissues (see Toole, 1976, for review). *In vitro* studies suggest HA promotes the invasion of embryonic cells into or through collagen gels (Bernanke & Markwald, 1984; Tucker & Erickson, 1984). For example, quail neural crest cells translocate at a significantly more rapid rate through collagen gels that contain low concentrations of HA than through gels of collagen alone (Tucker & Erickson, 1984), and HA opens spaces between the collagen fibrils in these gels (Turley *et al.* 1985). Since HA is a non-adhesive substratum for neural crest cells *in vitro* (Erickson & Turley, 1983; Tucker & Erickson, 1984), the promotion of cell migration into gels containing low concentrations of HA is probably due to the opening of spaces in the collagen gel.

In both *Xenopus* and young *Discoglossus* embryos, the lateral pathway is filled with collagen fibrils coated with RR-positive spherical aggregates believed to be CS proteoglycan. Neural crest cells avoid migrating into this pathway in *Xenopus* unless the ECM has been experimentally treated with CH ABC, and in *Discoglossus* until the volume of the pathway has increased. CS proteoglycan may be inhibiting the migration of neural crest cells through the lateral pathway by one of two mechanisms. (1) CS proteoglycan may be acting as a cement, glueing the ectoderm to the somites so tightly as to prevent the migration of cells through the ECM by mechanical obstruction. This role for CS proteoglycan is supported by a number of observations. When the ectoderm of anaesthetized embryos is peeled away from the somites using tungsten needles, it is attached tenaciously to the apex of the somites, where the concentration of CS proteoglycan is the greatest. When melanophores are observed in the lateral pathway, they are along the intersomitic furrows, where more space would be available. (2) CS proteoglycan in the lateral pathway may be a less adhesive substratum than the ECM in the ventral pathway. This is supported by the observations that fewer RR-positive spherical aggregates are seen in the ECM of the ventral pathway (except in the sheath of the notochord), and that the melanophores occasionally seen in the lateral pathway remain associated with the somites (that are relatively free of CS proteoglycan) and not the ectoderm when the ectoderm is peeled away with tungsten needles. Furthermore, *in vitro* studies with avian neural crest have shown that CS proteoglycan is not an adhesive migratory substratum, and when added to relatively adhesive substrata such as FN, it reduces cell adhesion (Newgreen *et al.* 1982; Erickson & Turley, 1983). Similarly, *Xenopus* neural crest cells do not attach to

CS derivatized to the surface of plastic dishes (unpublished observations by the author). It is difficult to distinguish between these two roles of CS proteoglycan, and they are not mutually exclusive. For example, melanophores may migrate through the intersomitic furrows because the increased space gives the cells access to a substratum that is more adhesive than the CS proteoglycan-rich ECM associated with the ectoderm (see below).

Increases in extracellular space by HA in *Discoglossus* may be permitting pigment cell migration into the lateral pathway by one of two mechanisms. (1) Opening spaces may disrupt a physical barrier either produced by matrix between cells, or caused by the close apposition of different tissues. Anderson & Meier (1982) have shown that when spaces surrounding avian cranial neural crest are collapsed by injection of hyaluronidase before migration, neural crest cells still enter the pathway. This suggests that HA is breaking bonds between tissues lining the pathway, and that the actual space is not needed for migration. This idea is also supported by Fig. 4E,F, showing *Xenopus* melanophores, which are restricted from the ventral pathway, migrating through the very small spaces surrounding individual somite cells. This suggests that space itself is not a prerequisite for pigment cell migration, but the nature of the space (e.g. filled with a non-adhesive matrix component) must also be taken into consideration. It is important to remember, however, that melanophores are filled with non-deformable yolk platelets (Algard, 1953) when they enter the ventral pathway, and that these platelets are depleted when the cells migrate through the somites. The absence of yolk platelets later in development may permit the melanophores to invade smaller spaces. (2) When HA opens spaces in the lateral pathway of *Discoglossus*, as indicated by the concurrent increase in microfibrils in the ECM, pigment cells may enter the pathway because they are able to use the surface of the somites and developing capillaries as migratory substrata. Again, space *per se* is not the necessary factor for migration, but the exposure of a more adhesive substratum (the surface of the somites) than the CS-rich subectodermal ECM.

Melanophores are often associated with basal laminae (Erickson, 1985), suggesting that this ECM is a particularly adhesive migratory substratum. For example, basal laminae surround capillaries and the pronephric ducts, with which melanophores are associated in both *Discoglossus* and *Xenopus*. In *Xenopus*, the appearance of basal laminae around the muscle cells of the somite coincides with the invasion of this tissue by melanophores, suggesting that the appearance of this preferred substratum may guide pigment cells from the ventral pathway to the dermis.

GAG are not the only class of ECM macromolecules to have been implicated in guiding neural crest cell migration. The distribution of the adhesive glycoprotein fibronectin, which appears to be necessary for normal neural crest cell migration in the chick (Boucaut *et al.* 1984), could also define pathways of neural crest migration in amphibians. Preliminary studies (Krotoski & Bronner-Fraser, 1984) have shown that FN is found in the ventral, lateral, and dorsal neural crest migratory pathways of *Xenopus laevis*. The ubiquitous distribution of FN seems to

preclude its role in restricting melanophore migration to the ventral pathway. It is important, however, to remember that GAG interact with FN (Yamada, Kennedy, Kimata & Pratt, 1980; Turley *et al.* 1985) and may effectively mask its adhesive properties (Newgreen *et al.* 1982; Erickson & Turley, 1983), and in this way present a less adhesive substratum to cells in the lateral pathway of *Xenopus laevis*.

It is interesting to speculate about the adaptive significance of the behaviour of pigment cells during early development. When they are just a few weeks old, *Discoglossus* larvae develop a cryptic green coloration. Amphibians appear green due to the arrangement of pigment cells in the dermis: a layer of xanthophores filters short wavelengths of visible light, a deeper layer of melanophores absorbs longer wavelengths, and an intermediate layer of iridophores reflects the middle wavelengths (yellow-green) back to the observer (Taylor & Bagnara, 1972). Perhaps the orderly segregation of pigment cells is facilitated by the affinities of melanophores for basal laminae (i.e. the somites) and of xanthophores for the GAG-rich dermal ECM.

I would like to thank C. A. Erickson for encouragement and advice throughout this study, as well as C. Campanella, R. Harris, D. Kline, T. Smart, M. Tretiak and E. A. Turley for technical assistance. I would also like to thank P. B. Armstrong and T. J. Poole for critical reading of the manuscript. This research was supported by NIH Grant PHS-DE 05630 to C.A.E. and DHHS National Research Service Award GM 07377 to R.P.T.

REFERENCES

ALGARD, F. T. (1953). Morphology and migratory behavior of embryonic pigment cells studied by phase microscopy. *J. exp. Zool.* **123**, 499–521.

ANDERSON, C. B. & MEIER, S. (1982). Effect of hyaluronidase treatment on the distribution of cranial neural crest cells in the chick embryo. *J. exp. Zool.* **221**, 329–335.

BAGNARA, J. T., MATSUMOTO, J., FERRIS, W., FROST, S. K., TURNER, W. A., JR, TCHEN, T. T. & TAYLOR, J. D. (1979). Common origin of pigment cells. *Science, N.Y.* **203**, 410–415.

BERNANKE, D. H. & MARKWALD, R. R. (1984). Effects of two glycosaminoglycans on seeding of cardiac cushion cells in collagen-lattice cultures. *Anat. Rec.* **210**, 21–35.

BOUCAUT, J.-C., DARRIBÈRE, T., POOLE, T. J., AOYAMA, H., YAMADA, K. M. & THIERY, J. P. (1984). Biologically active synthetic peptides as probes of embryonic development: A competitive peptide inhibitor of fibronectin function inhibits gastrulation in amphibian embryos and neural crest cell migration in avian embryos. *J. Cell Biol.* **99**, 1822–1830.

CAMPANELLA, C. & GABBIANI, G. (1980). Cytoskeletal and contractile proteins in coelomic oocytes, unfertilized and fertilized eggs of *Discoglossus pictus* (Anura). *Gamete Res.* **3**, 99–114.

DALTON, H. C. (1950). Inhibition of chromatoblast migration as a factor in the development of genetic differences in white and black axolotls. *J. exp. Zool.* **115**, 151–170.

DERBY, M. A. (1978). Analysis of glycosaminoglycans within the extracellular environments encountered by migrating neural crest cells. *Devl Biol.* **66**, 321–336.

DERBY, M. A. & PINTAR, J. E. (1978). The histochemical specificity of *Streptomyces* hyaluronidase and chondroitinase ABC. *Histochem. J.* **10**, 529–547.

DUBAND, J. L. & THIERY, J. P. (1982). Distribution of fibronectin in the early phase of avian cephalic neural crest migration. *Devl Biol.* **66**, 321–336.

DUSHANE, G. P. (1935). An experimental study of the origin of pigment cells in amphibia. *J. exp. Zool.* **72**, 1–31.

ELSDALE, T. & BARD, J. (1972). Collagen substrate for studies on cell behaviour. *J. Cell Biol.* **54**, 626–637.

EPPERLEIN, H. H. & CLAVIEZ, M. (1982*a*). Formation of pigment cell patterns in *Triturus alpestris* embryos. *Devl Biol.* **91**, 497–502.

EPPERLEIN, H. H. & CLAVIEZ, M. (1982*b*). Changes in the distribution of melanophores and xanthophores in *Triturus alpestris* embryos during their transition from the uniform to banded pattern. *W. Roux Arch. devl Biol.* **192**, 5–18.

ERICKSON, C. A. (1985). Control of neural crest cell dispersion in the trunk of the avian embryo. *Devl Biol.* (in press).

ERICKSON, C. A. (1986). Morphogenesis of the neural crest. In *Developmental Biology: A Comprehensive Synthesis* (ed. L. Browder). New York: Plenum Publishing Company. (in press).

ERICKSON, C. A. & TURLEY, E. A. (1983). Substrata formed by combinations of extracellular matrix components alter neural crest cell motility *in vitro*. *J. Cell Sci.* **61**, 299–323.

FISHER, M. & SOLURSH, M. (1979). The influence of the substratum on mesenchyme spreading *in vitro*. *Expl Cell Res.* **123**, 1–14.

HAY, E. D. (1978). Fine structure of embryonic matrices and their relation to the cell surface in ruthenium red-fixed tissue. *Growth* **42**, 399–423.

HAY, E. D. & MEIER, S. (1974). Glycosaminoglycan synthesis by embryonic inductors: neural tube, notochord, and lens. *J. Cell Biol.* **62**, 889–898.

HÖRSTADIUS, S. (1950). *The Neural Crest: Its Properties and Derivatives in the Light of Experimental Research.* London: Oxford University Press.

KELLER, R. E. & SPIETH, J. (1984). Neural crest cell behavior in white and dark larvae of *Ambystoma mexicanum*: Time-lapse cinemicrographic analysis of pigment cell movement *in vivo* and *in culture*. *J. exp. Zool.* **229**, 109–126.

KROTOSKI, D. & BRONNER-FRASER, M. (1984). Fibronectin distribution along neural crest pathways during *Xenopus laevis* development. *Soc. Neurosci. Abstr.* **10**, 763.

LE DOUARIN, N. (1982). *The Neural Crest.* New York: Cambridge University Press.

LE DOUARIN, N. M. & TEILLET, M. A. (1974). Experimental analysis of the migration and differentiation of neuroblasts of the autonomic nervous system and of neuroectodermal mesenchymal derivatives, using a biological cell marking technique. *Devl Biol.* **41**, 162–184.

LÖFBERG, J. & AHLFORS, K. (1978). Extracellular matrix organization and early neural crest migration in the axolotl embryo. *Zoon* **6**, 87–101.

LÖFBERG, J., AHLFORS, K. & FÄLLSTRÖM, C. (1980). Neural crest cell migration in relation to extracellular matrix organization in the embryonic axolotl trunk. *Devl Biol.* **75**, 148–167.

LUFT, J. H. (1971). Ruthenium red and violet: Chemistry, purification, methods of use for electron microscopy, and mechanism of action. *Anat. Rec.* **171**, 347–368.

MACMILLAN, G. J. (1976). Melanoblast-tissue interactions and the development of pigment pattern in *Xenopus* larvae. *J. Embryol. exp. Morph.* **35**, 463–484.

MAYER, B. W., JR, HAY, E. D. & HYNES, R. O. (1981). Immunocytochemical localization of fibronectin in embryonic chick trunk area vasculosa. *Devl Biol.* **82**, 267–286.

NEWGREEN, D. F., GIBBINS, I. L., SAUTER, J., WALLENFELS, B. & WÜTZ, R. (1982). Ultrastructural and tissue culture studies on the role of fibronectin, collagen and glycosaminoglycans in the migration of neural crest cells in the fowl embryo. *Cell Tiss. Res.* **221**, 521–549.

NEWGREEN, D. & THIERY, J.-P. (1980). Fibronectin in early avian embryos: Synthesis and distribution along migration pathways of neural crest cells. *Cell Tiss. Res.* **211**, 269–291.

NIEUWKOOP, P. D. & FABER, J. (1956). *Normal table of* Xenopus laevis (*Daudin*). Amsterdam: North Holland.

NODEN, D. (1975). An analysis of the migratory behavior of avian cephalic neural crest cells. *Devl Biol.* **42**, 106–130.

PINTAR, J. E. (1978). Distribution and synthesis of glycosaminoglycans during quail neural crest morphogenesis. *Devl Biol.* **67**, 444–464.

PRATT, R. M., LARSEN, M. A. & JOHNSTON, M. C. (1975). Migration of cranial neural crest cells in a cell-free hyaluronate-rich matrix. *Devl Biol.* **44**, 298–305.

ROVASIO, R. A., DELOUVÉE, A., YAMADA, K. M., TIMPL, R. & THIERY, J. P. (1983). Neural crest cell migration: Requirements for exogenous fibronectin and high cell density. *J. Cell Biol.* **96**, 462–473.

SAITO, H., YAMAGATA, T. & SUZUKI, S. (1968). Enzymatic methods for the determination of small quantities of isomeric chondroitin sulfate. *J. biol. Chem.* **243**, 1536–1542.

SINGLEY, C. T. & SOLURSH, M. (1980). The use of tannic acid for the ultrastructural visualization of hyaluronic acid. *Histochem.* **65**, 93–102.

STEVENS, L. C., JR (1954). The origin and development of chromatophores of *Xenopus laevis* and other anurans. *J. exp. Zool.* **125**, 221–246.

TAYLOR, J. D. & BAGNARA, J. T. (1972). Dermal chromatophores. *Amer. Zool.* **12**, 43–62.

THIERY, J. P., DUBAND, J. L. & DELOUVÉE, A. (1982). Pathways and mechanisms of avian neural crest cell migration and localization. *Devl Biol.* **93**, 324–343.

TOOLE, B. P. (1976). Morphogenetic role of glycosaminoglycans (acid mucopolysaccharides) in brain and other tissues. In *Neuronal Recognition* (ed. S. H. Barondes), pp. 275–329. New York: Plenum Press.

TOOLE, B. P. & TRELSTAD, R. L. (1971). Hyaluronate production and removal during corneal development in the chick. *Devl Biol.* **26**, 28–35.

TUCKER, R. P. & ERICKSON, C. A. (1984). Morphology and behavior of quail neural crest cells in artificial three-dimensional extracellular matrices. *Devl Biol.* **104**, 390–405.

TURLEY, E. A., ERICKSON, C. A. & TUCKER, R. P. (1985). The retention and ultrastructural appearances of various extracellular matrix molecules incorporated into three-dimensional hydrated collagen lattices. *Devl Biol.* **109**, 347–369.

TWITTY, V. C. (1936). Correlated genetic and embryological experiments on *Triturus*. I and II. *J. exp. Zool.* **74**, 239–302.

TWITTY, V. C. & BODENSTEIN, D. (1939). Correlated genetic and embryological experiments on *Triturus*. III. Further transplantation experiments on pigment development. IV. The study of pigment cell behavior in vitro. *J. exp. Zool.* **81**, 357–398.

VON DER MARK, H., VON DER MARK, K. & GAY, S. (1976). Study of differential collagen synthesis during development of the chick embryo by immunofluorescence. *Devl Biol.* **48**, 237–249.

WESTON, J. A. (1980). Role of the embryonic environment in neural crest morphogenesis. In *Current Research Trends in Prenatal Craniofacial Development* (ed. R. M. Pratt & R. L. Christiansen), pp. 27–45. New York: Elsevier/North Holland.

WESTON, J. A. & BUTLER, S. L. (1966). Temporal factors affecting localization of neural crest cells in the chicken embryo. *Devl Biol.* **14**, 246–266.

YAMADA, K. M., KENNEDY, D. W., KIMATA, K. & PRATT, R. M. (1980). Characterization of fibronectin interactions with glycosaminoglycans and identification of active proteolytic fragments. *J. biol. Chem.* **255**, 1181–1188.

(Accepted 12 September 1985)